Molecular and Cellular Biochemistry **222:** 97–106, 2001.

Differential zinc and DNA binding by partial peptides of human protamine HP2

Wojciech Bal,[1,2] Marcin Dyba,[1] Zbigniew Szewczuk,[1] Małgorzata Jeżowska-Bojczuk,[1] Jan Lukszo,[3] Gayatri Ramakrishna[2] and Kazimierz S. Kasprzak[2]

[1]*Faculty of Chemistry, University of Wroclaw, Wroclaw, Poland;* [2]*Laboratory of Comparative Carcinogenesis, National Cancer Institute at Frederick, Frederick, MD;* [3]*Peptide Analysis and Synthesis Unit, Research Technology Branch, National Institute of Allergy and Infectious Diseases, Rockville, MD, USA*

Abstract

The Zn(II) binding by partial peptides of human protamine HP2: $HP2_{1–15}$; $HP2_{1–25}$, $HP2_{26–40}$, $HP2_{37–47}$, and $HP2_{43–57}$ was studied by circular dichroism (CD). Precipitation of a 20-mer DNA by these partial peptides and the effects of Zn(II) thereon were investigated using polyacrylamide gel electrophoresis (GE). The results of this study suggest that reduced HP2 (thiol groups intact) can bind Zn(II) at various parts of the molecule. In the absence of DNA, the primary Zn(II) binding site in reduced HP2 is located in the 37–47 sequence (involving Cys-37, His-39, His-43, and Cys-47), while in the presence of DNA, the strongest Zn(II) binding is provided by sequences 12–22 (by His-12, Cys-13, His-19, and His-22) and 43–57 (His-43, Cys-47, Cys-53, and His-57). In its oxidized form, HP2 can bind zinc through His residues of the 7–22 sequence. Zn(II) markedly enhances DNA binding by all partial peptides. These findings suggest that Zn(II) ions may be a regulatory factor for sperm chromatin condensation processes. (Mol Cell Biochem **222**: 97–106, 2001)

Key words: protamine P2, protamine peptides, DNA, zinc, protamine-zinc binding

Introduction

DNA in vertebrate sperm is stabilized through the binding to protamines, small basic proteins rich in arginine, which provide positive charges required for the neutralization of DNA phosphates [1, 2]. In mammals, protamines also contain cysteine residues, which form intermolecular disulfide bridges, increasing the stability of the DNA-protein complex. Consequently, protamine-bound DNA in sperm head is compacted severalfold compared to somatic nuclei [3]. This function is exerted by protamine P1, expressed in all mammalian species. A few species, including mouse and man, express an additional protamine, P2, also containing histidine, [1, 2]. Strikingly, its presence at 50–70% of total protamine is required for male fertility in humans [4]. The sequence of human P2 (HP2) is as follows [1, 2]:

RTHGQ-SHYRR-RHCSR-RRLHR-IHRRQ-HRSCR-RRKRR-SCRHR-RRHRR-GCRTR-KRTCR-RH

Zn(II) binding in sperm chromatin is necessary for maintaining sperm viability [5]. HP2 is believed to provide these zinc binding site(s). A recent paper indicated that Zn(II) content of mammalian sperm cells (including human) correlates with protamine 2 abundance and it is sufficient in the majority of cases to form 1:1 complex with P2 [6]. The identity and localization of this site(s) within HP2 is, however, uncertain. One proposal, based on the effects exerted by Zn(II) on HP2 CD spectrum and structure prediction algorithms, suggests that two Zn(II) ions are coordinated to four separate histidine nitrogens each, producing multiple loops in the HP2 molecule [7]. This suggestion, neglecting the participation of Cys sulfur donors in the binding, is contrary to known coordination

Address for offprints: W. Bal, Faculty of Chemistry, University of Wroclaw, F. Joliot-Curie 14, 50-383 Wroclaw, Poland

preferences of Zn(II). The other proposal, based on Co(II) substitution and UV-vis spectra, suggests a single Cys2/His2 binding site, more or less analogous to zinc-finger domains [8]. Such a coordination set is chemically viable, but the criteria of selection of the particular coordinating residues out of many available (two out of nine His and two out of five Cys side chains) are not clear. Our preliminary study, using CD spectroscopy, indicated that HP2 may bind two Zn(II) ions *in vitro* with a relatively high affinity [9].

Human protamine HP2 possesses another metal-binding domain. It is the N-terminal tripeptide Arg-Thr-His, a specific Cu(II)- and Ni(II)-binding site, analogous to the physiological Cu(II) carrier in human serum albumin, and also involved in nickel toxicity [10]. In our recent studies of Cu(II) and Ni(II) interactions with HP2, we used its N-terminal pentadecapeptide ($HP2_{1–15}$) as a functional model. We have shown that the binding of either of these metal ions is very strong and specific [11]. Also, the Ni(II) complex can activate oxygen and hydrogen peroxide, leading to the oxidative damage of DNA and the peptide itself [12, 13], while the activity of the Cu(II) complex is limited to peptide destruction. In a subsequent work, we used NMR to elucidate the structure of the Ni(II) complex of $HP2_{1–15}$ [14]. We found that the Ni(II) binding results in long-range peptide structuring, which may be responsible for the enhancement of DNA binding and precipitation upon the N-terminal metal ion coordination, seen previously [12, 13].

Previous studies suggested that the Zn(II) binding has no effect on HP2-DNA interactions [15]. Taking into account the essentiality of Zn(II) for sperm viability on the one hand, and clear enhancement of DNA-$HP2_{1–15}$ binding by Cu(II)/Ni(II) on the other hand, we have decided to reanalyze this issue. We undertook an attempt to localize the Zn(II) binding site(s) within the HP2 molecule in the absence and presence of DNA. The multiplicity of potential Zn(II) donor groups, combined with an absence of a secondary structure, makes the identification of the actual binding site(s) a very difficult task. We assumed, based on previous CD studies [7, 9] that the highly charged HP2 molecule (+29 per 57 residues, from arginine and lysine side chains) would maintain an extended conformation, as the one minimizing electrostatic repulsion. Therefore, the most likely binding sites would be formed locally, involving four consecutive His and/or Cys donor groups. His/Cys metal binding domains are most specific to Zn(II) when the binding is provided by two Cys and two His residues, and such domains are most frequently encountered in DNA binding [16, 17]. Therefore, we decided to dissect the HP2 sequence into five partial peptides containing such residues, and to study their properties comparatively.

Cys residues are present in HP2 in positions 13, 29, 37, 47 and 54. We assumed that Cys-13 is too distant from Cys-29 to be combined in the same peptide. On the other hand, it is surrounded by many His residues; thus the selection of peptides A ($HP2_{1–15}$) and B ($HP2_{1–25}$). The other four Cys residues could be combined in three sequential pairs, allowing for the design of three partially overlapping peptides: C ($HP2_{26–40}$), D ($HP2_{37–47}$), and E ($HP2_{43–57}$). Each of them contains just two His residues. In this way each of our partial peptides provided just one potential Zn(II) binding site with a Cys/His3 or Cys2/His2 donor set. We synthesized these peptides and studied their Zn(II) binding properties in the absence and presence of a short double-stranded oligonucleotide to create a dataset that should allow to propose the localization of one or more Zn(II) binding sites in the whole HP2. This paper presents the results of our studies.

Materials and methods

Materials

$ZnCl_2$ (99.99% purity) was purchased from Aldrich (Milwaukee, WI, USA). Other simple chemicals were obtained from Sigma Chemical Co. (St. Louis, MO, USA) or E. Merck (Darmstadt, Germany).

Peptide synthesis

Peptides $HP2_{1–15}$ (A), $HP2_{1–25}$ (B), and $HP2_{26–40}$ (C) were synthesized by Fmoc strategy [18] on a solid support, using an Applied Biosystems Inc. (ABI, Foster City, CA, USA) model 430A automated peptide synthesizer. The substrates, N-Fmoc protected amino acids, Fmoc-amide resin, and all other peptide synthesis reagents were obtained from ABI. Acetylation of the N-terminal was performed using N-acetylimidazole (Sigma) in dimethylformamide. Peptides $HP2_{37-47}$ (D) and $HP2_{43-57}$ (E) were also synthesized by Fmoc strategy on a solid support, but using a manual setup. Materials for theses syntheses were obtained from Calbiochem-Novabiochem AG, Läufelfingen, Switzerland (N-Fmoc protected amino acids, amide MBHA resin, Fmoc-Cys Wang resin and benzotriazol-1-yl-oxy-tripyrrolidinophosphonium hexafluorophosphate (PyBOP)), and Sigma or Riedel-deHaën GmbH, Seeize, Germany) (other standard peptide synthesis reagents). Cleavage was effected on a 0.25 mmol scale, using a mixture of trifluoroacetic acid (TFA), thioanisole and ethanedithiol (v/v/v = 92/5/3), over a period of 2 h for automated synthesis or on a 0.05 mmol scale, using a mixture of trifluoroacetic acid (TFA), phenol, water, thioanisole and triisopropylsilane (v/v/v/v/v = 80/5/5/5/5), over a period of 9 h for manual synthesis. The crude peptides were purified by preparative HPLC on the Waters Delta Pak (Waters, Milford, MA, USA) C_{18} column, 300 Å pore size, 15 μm particle size, 19 × 300 mm, eluting with 0.1% TFA/water (solvent A) and 0.1% TFA/80% acetonitrile/water (solvent B), using a gradient of 5–25% B/

40 min at a flow rate of 12.5 mL/min with detection at 215 nm. Fractions collected across the main peak were assessed by HPLC analysis on a Rainin Dynamax (Ridgefield, NJ, USA) C_{18}, 300 Å, 5 μm, 4.6 × 250 mm column, using gradient of 0%–35% B over 20 min, flow rate of 1 mL/min and detection at 215 nm. Correct fractions were pooled and lyophilized to yield white solids of purity exceeding 95% as assessed by HPLC analysis of the final materials. Identity of all peptides was confirmed by mass spectrometry, utilizing a Voyager RP MALDI-TOF instrument from PerSeptive Biosystems, Inc. (Framingham, MA, USA).

While the four shorter sequences were found to be homogenous, the longer, very basic peptide B was still contaminated by the truncated sequences missing one or more arginine residues. That peptide was further purified by a semi-preparative HPLC on an ion exchange column (PolyCAT A; 300 Å, 5 μm, 4.6 × 200 mm) from The Nest Group, Inc. (Southborough, MA, USA), eluting with 10 mM ammonium acetate/10% acetonitrile/water (solvent A) and 10 mM ammonium acetate/1 M sodium perchlorate/10% acetonitrile/water (solvent B), using a gradient of 35–100% B/35 min at a flow rate of 4 mL/min with detection at 220 nm. Fractions collected across the main peak were assessed by HPLC analysis on the same column and solvent system, at the flow rate of 1 mL/min. Correct fractions were pooled and desalted by preparative HPLC on the Waters Delta Pak C_{18} column, same as above, eluted with 0.1% TFA/water (solvent A) and 0.1% TFA/80% acetonitrile/water (solvent B), using a gradient of 5–35% B/40 min at a flow rate of 12.5 mL/min with detection at 215 nm. Fractions collected across the main peak were pooled and lyophilized to yield a white solid of purity exceeding 95% as assessed by HPLC and MALDI-TOF MS analysis.

Oligonucleotide synthesis

The complementary 20-mer oligodeoxynucleotides, 5′-GGAGGCGTCCGGTTCCAATA-3′ (SS1) and 5′-TATTGGAACCGGACGCCTCC-3′ (SS2) were obtained purified from SAIC-Frederick and annealed to form a double-stranded 20-mer nucleotide (DS). The annealing occurred with a 100% efficacy. However, the final preparation contained an 18% surplus of SS1 and was used as such. This composition appeared to be advantageous by allowing us to make comparisons of peptide binding to the two forms of DNA in single experiments.

Potentiometry

The protonation constants of the peptides in the presence of 0.1 M KNO_3 were determined at 25ºC using pH-metric titrations over the pH range 3–11 (Molspin automatic titrator, Molspin Ltd., Newcastle-upon-Tyne, UK) with NaOH as titrant. Changes in pH were monitored with a combined glass-calomel electrode calibrated daily in hydrogen concentrations by HNO_3 titrations [19]. Sample volumes of 1.5 mL and peptide concentrations of 0.3–0.5 mM were used. All measurements were performed under argon. The data were analyzed using the SUPERQUAD program [20].

CD spectra

The spectra were recorded on a Jasco J-720 spectropolarimeter (Japan Spectroscopic Company, Hiroshima, Japan) in the spectral range of 190–350 nm, for 2.5–10 μM peptides dissolved in 10 mM sodium phosphate buffer, containing 20 μM DTT. Without the latter, the spectra could not be measured due to autooxidation and precipitation of the peptides under ambient atmosphere. Duplicate runs were averaged to reduce measurement noise at short wavelengths.

Gel electrophoresis

The samples dissolved in the modified TB running buffer (90 mM Tris-borate, pH 7.4, no EDTA) containing oligonucleotides, 1 μM DS and 0.18 μM SS1 (high concentration) or 0.4 μM DS and 0.072 μM SS1 (low concentration) and combinations of various concentrations of HP2 partial peptides and Zn(II) in a total volume of 12 μL were incubated for 15 min, mixed with 2 μL of loading buffer (30% Ficoll and 0.05% bromophenol blue and xylene cyanol in 10 × running buffer) and loaded on Novex Pre-Cast 12% polyacrylamide gels (Invitrogen, Carlsbad, CA, USA). The electrophoresis was run for 2 h at 120 V, using the running buffer. In some experiments, the samples also contained 0.5 mM DTT. The gels were stained with ethidium bromide (Bio-Rad, Hercules, CA, USA) and photographed and processed with an IS-1000 Digital Imaging System (Alpha Innotech Corp., San Leandro, CA, USA). DNA in individual lanes was quantified using reference lanes of untreated oligonucleotides, present in each gel.

Results

Potentiometry

Protonation constants of peptides A, C, D and E are presented in Table 1. Peptide B was not measured because we were not able to obtain it in amounts required by potentiometry. Average values of protonation constants of His residues are also presented in Table 1.

Table 1. Protonation constants of HP2 partial peptides in 0.1 M KNO_3 at 25°C (pK values)[a]

Peptide	His_1	His_2	His_3	Cys_1	Cys_2	Average His	Other
A	5.48	5.90	6.47		8.33	5.95	7.13[b], 9.83[c]
C	5.64	6.56		7.67	8.82	6.10	9.97[d]
D	5.45	5.94		7.56	8.15	5.70	6.54[b]
E	5.38	5.97		6.83	8.67	5.68	11.06[d]

[a]S.D. based on statistical error distributions yielded by SUPERQUAD are within 0.01–0.02 log units; [b]terminal amine; [c]Tyr phenol; [d]Lys side-chain amine.

Circular dichroism

In order to measure the Zn(II) binding to protamine partial peptides directly, CD spectra of peptides A–E, dissolved in 10 mM sodium phosphate buffer containing 20 μM DTT were recorded in the presence of increasing amounts of Zn(II), until the saturation of spectral changes. DTT, an efficient peptide thiol reductant [21], was used to preserve peptide thiols in their reduced state and thus assure peptide solubility. Two saturable effects were seen in the spectra (Fig. 1): a decrease and a slight redshift of the short wavelength spectral minimum, and the appearance of a new, positive band at ca. 220 nm. These two effects allowed for the construction of two independent titration curves for each peptide, from which log K_c values (conditional constants for pH 7.4, which ignore peptide protonation) for ZnP complexes (P = A, B, C, D, E), were calculated. These constants take into account the competition for Zn(II) binding from DTT [22] and phosphate [23]. Formal stability constants (β) were obtained from K_c values using potentiometry-derived protonation constants for the peptides. Both are presented in Table 2.

The log K_c values may be somewhat overestimated due of uncertainties in actual concentrations of reduced DTT, e.g. a 2-fold decrease of DTT concentration results in a decrease of the calculated log K_c value by 0.2–0.4 units. The curves for peptides B, D and E did not exhibit deviations from the 1:1 binding model. On the contrary, an apparent increase of log K_c values was found for initial titration points for peptides A and C. This may be interpreted as formation of 2:1 peptide-to-zinc complexes at high peptide surplus over free Zn(II) ions. These points were not used in the calculations of K_c values.

Gel electrophoresis

The binding of HP2 partial peptides to DS and SS1 oligonucleotides was studied by polyacrylamide gel electrophoresis. Two oligonucleotide concentrations were used: 1 μM DS + 0.18 μM SS1 (high concentration) or 0.4 μM DS + 0.072 μM SS1 (low concentration). In order to correlate the

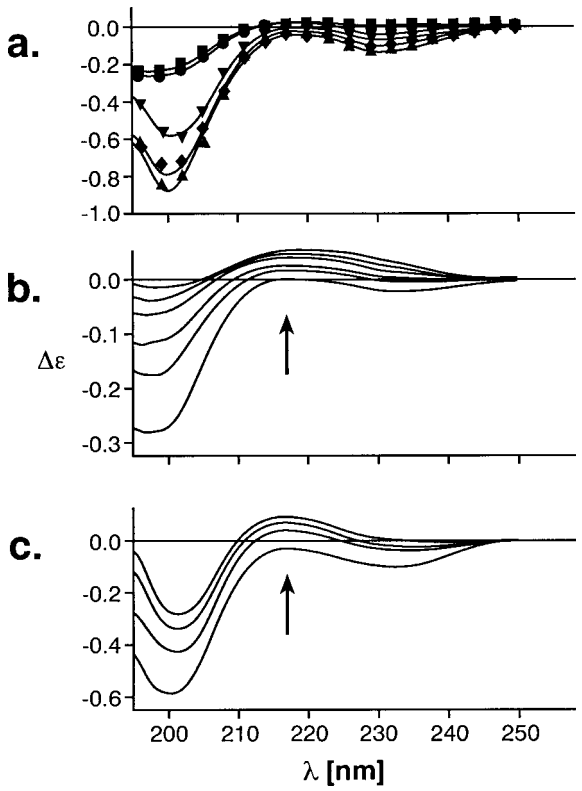

Fig. 1. CD of HP2 partial peptides (2.5–10 μM) in 10 mM Na phosphate buffer, pH 7.4. Arrows indicate the directions of spectral changes upon Zn(II) additions. (a) Spectra in the absence of Zn(II): ■, peptide A; ●, peptide B; ▲, peptide C; ▼, peptide D; ◆, peptide E. (b) Zn(II) titration of peptide B (0–4 mol equivalents of Zn(II), 0.8 mol equivalent steps). (c) Zn(II) titration of peptide D (0–3 mol equivalents of Zn(II), 1.0 mol equivalent steps).

redox status of the thiol groups of the peptides with their DNA binding abilities, the experiments were done in the presence and absence of DTT. The nucleotide mixtures were incubated with varying amounts of individual peptides for 15 min, then loaded onto gels and analyzed. In all cases only the free (soluble) oligonucleotides, migrating in the gel, and not their non-migrating peptide complexes (insoluble), were measured. Examples of the gels are presented in Fig. 2, and examples of the titration curves obtained from them by densitometry are presented in Fig. 3. It was uniformly found that the titration curves for SS1 followed those for DS, indicating the same affinities of both forms of DNA to the individual reduced peptides. The sigmoidal curves obtained were very similar to those seen by Bianchi *et al*. in their study of HP2 binding to DNA fragments of various lengths [15]. These authors demonstrated that the binding of HP2 to DNA caused precipitation of the resulting complex. Their results, obtained using DNA fragments much longer than ours, indicated that the precipitation occurred at the arginine/phosphate ratio of 1.2, independently of the length of DNA. This interpretation does not allow for calculation of binding constants. We ob-

Table 2. Conditional stability constants (K_c)[a] at pH 7.4 and overall stability constants (β)[b] of Zn(II) complexes with HP2 partial peptides, calculated from CD spectra

Peptide	log K_c (minimum)[c]	log K_c (CT)[c]	Average log K_c	Log β_{MHP}	Log β_{MP}
A	6.0(1)[d]	6.0(2)	6.0(2)	17.0	7.2
B	7.0(1)	7.1(3)	7.1(3)	–	–
C	4.9(4)	5.4(2)	5.2(4)	17.1	7.1
D	7.6(1)	7.8(4)	7.7(3)	–	8.9
E	6.0(2)	5.9(2)	6.0(2)	18.5	7.4

[a]$K_c = [MP]/[M][P]$; where [MP] is the total molar concentration of the metal-peptide complexes; [M] is the molar concentration of uncomplexed metal; [P] is the total concentration of uncomplexed peptide in its all protonation states; [b]$\beta = [MH_nP]/[M][H]^n[P]$; [c]From the minimum and charge transfer (CT) wavelengths, respectively; [d]S.D. of the last digit are given in parentheses.

served DNA precipitation at the excess of peptide charges over DNA phosphates higher than 1.2 (see Fig. 3). High ionic surplus of peptide in the precipitate is impossible for electrostatic reasons. One possible explanation is based on an assumption that the titration curves represent an equilibrium phenomenon that can be described by a binding constant of some kind.

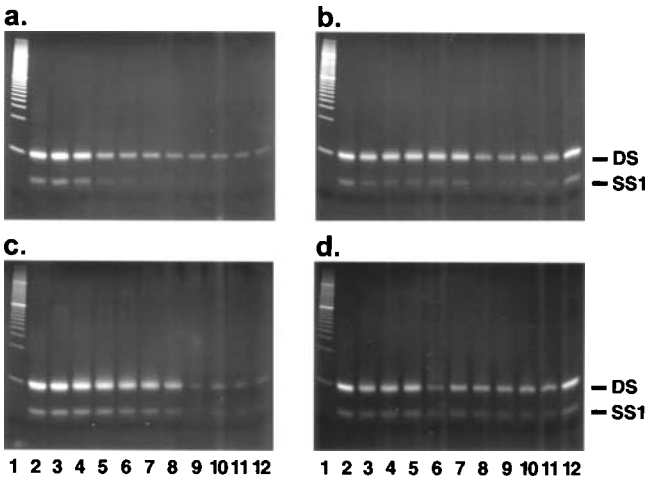

Fig. 2. Examples of polyacrylamide gels of DNA interactions with HP2 partial peptides and Zn(II). (a) DNA titration with peptide D in the absence of DTT. Lane 1: DNA molecular weight markers; lane 2: DNA control (1 μM DS + 0.18 μM SS1); lanes 3–12: DNA as in lane 2, with incrementally increasing amounts of peptide D, from 2.95–29.5 μM. (b) DNA titration with Zn(II) in the presence of peptide D and the absence of DTT. Lane 1: DNA molecular weight markers; lane 2: DNA control (1 μM DS + 0.18 μM SS1); lane 3: DNA as in lane 2, with 14.75 μM peptide D; lanes 4–11: DNA and peptide D as in lane 3, with increasing amounts of Zn(II): 1, 2, 10, 20, 50, 100, 150, 200 × 8.33 μM, respectively; lane 12: DNA as in lane 2, with Zn(II) as in lane 11 (1.67 mM). (c) DNA titration with peptide A in the presence of DTT. Lane 1: DNA molecular weight markers; lane 2: DNA control (1 μM DS + 0.18 μM SS1); lanes 3–12: DNA as in lane 2, with incrementally increasing amounts of peptide A, from 2.9–29 μM. (d) DNA titration with Zn(II) in the presence of peptide A and DTT. Lane 1: DNA molecular weight markers; lane 2: DNA control (1 μM DS + 0.18 μM SS1); lane 3: DNA as in lane 2, with 8.7 μM peptide A; lanes 4–11: DNA and peptide A as in lane 3, with increasing amounts of Zn(II): 1, 2, 10, 20, 50, 100, 150, 200 × 8.33 μM, respectively; lane 12: DNA as in lane 2, with Zn(II) as in lane 11 (1.67 μM).

The attempts to analyze the titration curves in this way presented difficulties. We found just one formula that yielded consistent values of constants for any (and all) of the peptides in both the absence and presence of DTT. This formula represents a modified solubility product (K_{so}), with the peptide concentration in the first power instead of (formally appropriate) stoichiometric coefficient derived from the peptide charge (between 4 and 8 for individual peptides):

$$K_{so} = [DS]_{free} \times [P]_{free} \text{ (P = A, B, C, D, or E)}$$

The K_{so} values were consistent between high and low concentration experiments, supporting the validity of this approach. We might also presume that the alternative cause of the observed deviation from the approximate 1:1 charge stoichiometry could be coprecipitation of very high amounts of the buffer anion (borate) with the DNA-peptide complex. However, if this were true then such coprecipitation would systematically decrease the K_{so} values at lower concentrations of peptides and DNA; but this was not observed.

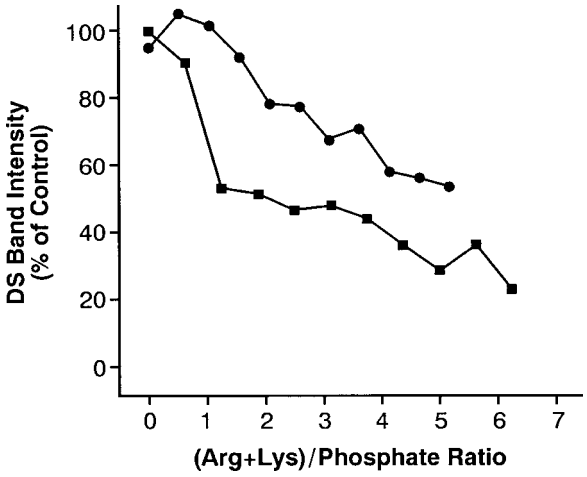

Fig. 3. Examples of quantification of gel electrophoresis titrations of DS DNA (0.4 μM) with HP2 partial peptides in the presence of DTT: ■, peptide B; ●, peptide C.

From the electrostatic neutrality condition, the stoichiometry of the DNA-peptide complex should be based on the balance of positive peptide charges and negatively charged DNA phosphates (40 for DS). Bianchi et al. included only Arg residues as charged at neutral pH [15]. In fact, Lys residues, which are charged at pH 7.4, should also be included. The question was open for His residues, which are relatively acidic in HP2 partial peptides (Table 1), with average pK_a values below 6. This might, however, change in the vicinity of a highly negatively charged oligonucleotide, making His side chains effective DNA binding sites [24]. The calculations were done for all these possibilities. We found that in our experimental conditions of high molar peptide excess over oligonucleotides, the inclusion of His side chains had a negligible impact on calculations of K_{so} values (increase by less than 0.05 log units, well within the S.D.) The presence of SS1 in our DS preparation was taken into account in the calculations by assuming identical K_{so} values (as indicated directly by titration curves) and using the precipitate stoichiometry provided by the electroneutrality principle. The log K_{so} values thus obtained for reducing (with DTT) and oxidizing (without DTT) conditions are presented in Table 3. Figure 4 shows the relationship between the peptide charge (taken as number of Arg and Lys residues) and log K_{so}. Note that in reducing conditions, the dependence of log K_{so} value on peptide charge is perfectly linear (R = 0.996). In the absence of DTT, this linearity is lost.

Another set of gel electrophoresis experiments was aimed at estimating the effect of Zn(II) on the interaction of HP2 partial peptides and oligonucleotides. These were performed as Zn(II) titrations of oligonucleotide-peptide mixtures, using peptide excess that previously precipitated of 10–20% of the added DNA. In all cases titration curves had sharp sigmoidal shapes (see Fig. 5 for examples). The enhancement of DNA precipitation was invariably seen for higher Zn(II) concentrations. In some cases, the concentration of free oligonucleotide fell below the detection limit. This effect was absent in the absence of peptides (lanes 12 of Zn(II) titration gels). The appropriate log K_{so} values at Zn(II) saturation, compared to Zn(II)-free situation (or their lower limits when DNA was precipitated out) are presented in Table 3.

Table 3. Log K_{so} values determined for oligonucleotide precipitation by HP2 partial peptides (free) and their Zn(II) complexes in the absence and presence of DTT[a,b]

Peptide	DS		DS/DTT	
	Free	Δ Zn	free	Δ Zn
A	–11.8(2)	1.2(5)	–11.5(3)	0.5(2)
B	–12.2(4)	1.4(3)	–12.1(2)	> 1.8
C	–12.3(3)	> 1.6	–12.0(2)	> 2.3
D	–11.9(2)	0.4(1)	–11.6(2)	1.2(6)
E	–12.5(2)	2.1(4)	–11.9(2)	> 2.0

[a]Δ Zn = log K_{so} (free) – log K_{so} (Zn); [b]S.D. on the last digit are given in parentheses.

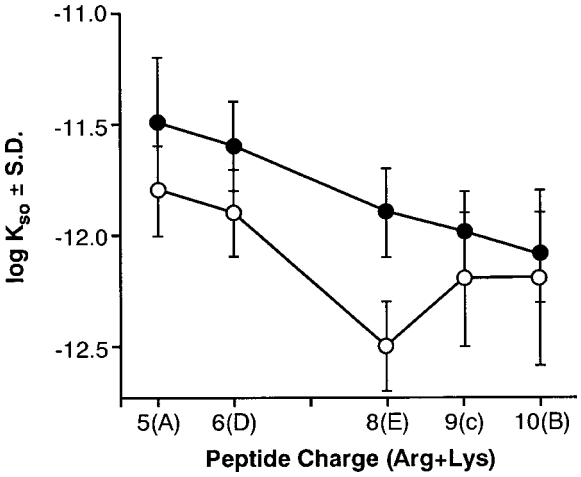

Fig. 4. The dependence of log K_{so} values of peptide-DS DNA complexes on peptide charge: ■, with DTT; O, without DTT.

The results of gel electrophoresis experiments did not allow to calculate meaningful binding constants because of a possibility for free Zn(II), DTT, and their complexes to diffuse out of the gel wells (and thus change the equilibrium) just after loading. However, the experiments were fully reproducible. Therefore, the relative orders of Zn(II) affinities to the DNA complexes with various peptides could be established using values of total Zn(II) concentration at titration mid-points (Fig. 5). They are presented in Table 4 in comparison with affinity orders for peptide-DNA and Zn(II)-peptide interactions.

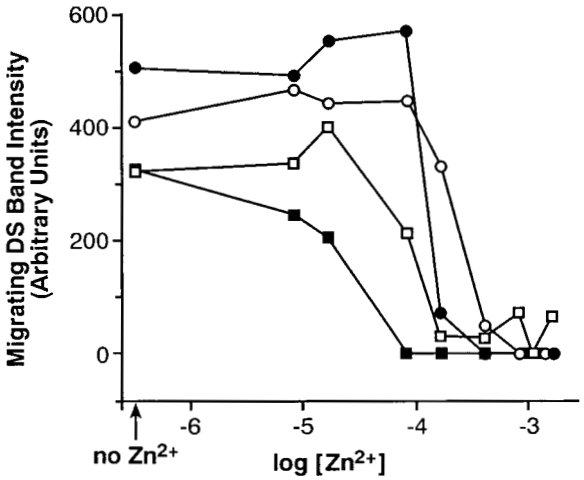

Fig. 5. Examples of the effects of Zn(II) on DS precipitation by HP2 partial peptides (expressed as the amount of DS migrating in the gel); ■, peptide B with DTT; ●, peptide C with DTT; □, peptide B without DTT; O, peptide C without DTT.

Discussion

Zn(II) binding to partial peptides in the absence of DNA

CD titrations were evaluated using two mutually independent, direct features of Zn(II) coordination to the peptides. The minimum at 200 nm, which decreased in the presence of increasing amounts of Zn(II), originates in coupled peptide carbonyl chromophores and reflects the overall conformation of the peptide's main chain [25]. Analogous decreases of such bands were seen previously in Zn(II) titrations of the whole HP2 [7, 9], as well as zinc finger proteins [26, 27]. The maximum at 220 nm, which appeared upon Zn(II) addition to each of the peptides studied in this work, is a charge transfer (CT) band of the Zn(II)-S bond [27, 28]. Therefore, these spectral changes reflected the peptide folding due to multidentate Zn(II) binding, as well as specific contributions to the binding from thiolates. As shown in Table 2, both effects independently yielded the same values of K_c, thus assuring that the formation of zinc binding domains was really measured.. Peptide D provided the strongest Zn(II) binding, with log K_c of 7.7; peptide B came second with log K_c of 7.0; and the remaining HP2 partial peptides bound Zn(II) much more weakly. Interestingly, there was no preference for 2Cys/2His (C, D and E) over 3His/Cys sites (A and B). The presence of the CT band at 220 nm assures Cys sulfur usage by peptide B for Zn(II) binding and excludes an alternative His4 coordination. The values found for HP2 partial peptides are much below the lower limit of log K_c values measured for regular zinc fingers, 9–12 [16, 17, 26, 29-31]. This is likely due to the electrostatic repulsion from many charged Arg residues, counteracting the peptide folding required for tetradentate Zn(II) coordination as opposed to cooperative protein folding present in typical zinc fingers [17]. Our results correspond well with the affinity constants obtained for HP2, equal to 7.1 (log K_c for the primary site) and 5.6 (log K_c for the secondary site) [9]. The two highest log K_c values for partial peptides are 7.7 and 7.0. Noting that these values may be somewhat overestimated, and that the electrostatic repulsion should be stronger in the whole peptide than in its fragments, the localization of the primary Zn(II) site of HP2 within peptide D is more than likely. Our results also suggest that the secondary Zn(II) binding site is localized in peptide B. It can *a priori* contain any three of five His residues (the involvement of Cys-13 residue was confirmed directly). The 1 log unit enhancement of binding compared to peptide A suggests that His-19 and/or His-22 belong to the binding site. Assuming its sequentiality, it may be composed of either His-12, Cys-13, His-19, and His-22, or His-7, His-12, Cys-13, and His-19. The Zn(II) complex of peptide B may be a mixture of both. The +1 charge of the Zn(II) site, resulting from the 3His/Cys coordination mode, less favorable in the highly charged whole HP2, may be responsible for the stability difference between it and peptide B.

According to a previous proposal [8], Zn(II) should bind to two Cys donors from our peptide E (Cys-47 and Cys-54) along with two His donors from peptide B (His-19 and His-22). Our results indicate that peptide D offers a much higher zinc-binding affinity than peptide E, and thus do not support that proposal.

Table 4. Relative affinity orders for HP2 partial peptides interactions with DNA and Zn(II) in the absence and presence of DTT[a]

Components	DS	DS/DTT
Zn + P + DNA; Zn binding	B ≥ A >> C ≥ D > E	B = E > D > A >> C
Zn + P + DNA; Zn enhancement of DNA precipitation	E ~ C > B > A > D	E ~ C ~ B > D > A
Zn + P	–	D > B >> A = E > C
P + DNA	E > B = C > D ≥ A	B ≥ C ≥ E > D ≥ A

[a] ≥, difference within S.D.; ~, probably of similar magnitude; >, difference within 1 log unit; >>, difference higher than 1 log unit.

DNA interaction with partial peptides of HP2

DNA binding is the fundamental physiological function of HP2. We aimed at gaining insight into the details of this interaction by studying the binding of its partial peptides to a short oligonucleotide. We hoped that its small size would prevent precipitation seen in previous studies of the whole HP2 [15] or $HP2_{1–15}$ [12, 13] binding to DNA of various sizes. This failed, as DNA precipitation was the only effect we could measure. Nevertheless, valuable information was obtained. Table 3 presents the apparent solubility products calculated from gel electrophoresis experiments performed at reducing (DTT present) and oxidizing (DTT absent; ambient atmosphere) conditions. Note that the K_{so} values obtained by us are valid only for our particular experimental settings, and are used here only for comparative purposes.

Under the reducing conditions, the precipitating capacity of the peptides is a linear function of the number of their positively charged arginine and lysine residues (Fig. 4). Arginines and lysines are distributed differently in the sequences of particular partial peptides, and so the adoption of any non-extended conformation would result in deviations from the linearity observed. This finding is in agreement with models of DNA binding by various protamines in the absence of Zn(II) [32-34]. The linearity is lost in the absence of DTT, but the binding becomes somewhat stronger, by ca. 0.3 log units on average, apparently due to the formation of intra- and/or intermolecular disulfide bridges. Such enhancement has been relatively highest for peptide E, which correlates with a low pK value for one of its cysteines (Table 1), bearing in mind that thiols are oxidized to disulfides as anions [35]. This effect corresponds to the process of sperm chromatin condensation by the formation of disulfide bridges.

Zn(II) interactions with peptide-DNA complexes

The titrations of the oligonucleotide/peptide mixtures with Zn(II) showed that, at sufficient excess, Zn(II) is able to enhance DNA precipitation by all the investigated peptides. This enhancement typically exceeded 1 log unit of apparent K_{so} in both the presence and absence of DTT (Table 3). The Zn(II) titration curves exhibited very sharp sigmoidal shapes (Fig. 5). Such effect is characteristic for two-state systems and thus indicates the formation of specific peptide-Zn(II)-DNA complexes, which are less soluble (i.e. stronger) than the parent peptide-DNA aggregates. Zn(II) added to peptide-free DNA at the highest concentration used in titrations did not cause DNA precipitation, nor affected its mobility (Fig. 2, lane 12 in all Zn(II) titration gels), indicating that Zn(II) binds to the peptide rather than the DNA part of peptide-DNA complexes. Zn(II) affinities to peptide-DNA complexes could be ordered using total Zn(II) concentrations at transition midpoints, thus providing insight into Zn(II) binding preferences in the DNA-bound peptides (Table 4). Peptides B and E provide strongest Zn(II) binding for reducing conditions. Peptide B remained dominant for oxidizing conditions, while E lost its binding capabilities due to sulfur oxidation. The total Zn(II) concentrations at transition midpoints were lower in the presence of DTT even though a large proportion of Zn(II) was sequestered by the latter. Therefore, Zn(II) binding involving Cys residues was much stronger than with His residues only. Peptide specific Zn(II) effects on DNA binding suggest that peptide-Zn(II) complexes retain specific, partially folded, conformations in the presence of DNA. Interestingly, these complexes precipitate DNA more efficiently than free peptides, with stoichiometries approaching the1:1.2 value found previously for the whole HP2 [15].

We have obtained relative Zn(II) affinities for individual peptides covering the whole sequence of HP2 for reduced, DNA-free conditions, as well as for the reduced and oxidized DNA-bound states. Our results suggest that Zn(II) may bind at various sites in HP2, depending on external conditions. These possibilities are presented graphically in Fig. 6.

Kvist *et al*. demonstrated the importance of Zn(II) bound to thiols in sperm chromatin for maintaining sperm viability [5, 36–39]. In particular, the Zn(II) level in sperm head increases upon ejaculation as a result of Zn(II) transfer from prostatic fluid [36]. Balhorn and coworkers studied the roles of HP1 and HP2 in DNA condensation, including formation of intra- and intermolecular disulfide bridges [40–43] and recently showed that Zn(II) was abundant enough to bind whole HP2 in human sperm at a 1:1 stoichiometry [6]. Our results suggest that Zn(II) binding to HP2 in sperm chromatin may be heterogeneous, depending on the involvement of particular Cys residues in the disulfide formation, and on DNA binding. The enhancement of DNA binding by HP2 partial peptides in the presence of Zn(II) indicates that Zn(II) ions may play a regulatory role in specific structuring of sperm chromatin.

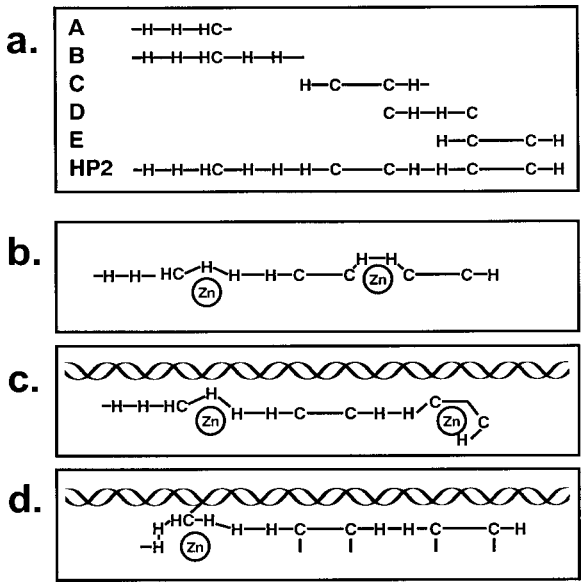

Fig. 6. A proposal of patterns of Zn(II) binding to HP2 at various conditions. Two highest affinity binding sites are shown for reduced HP2, and one for oxidized HP2, where binding constants are much lower. See text for details. (a) Schematic representation of the peptides; (b) Reduced HP2 in the absence of DNA; (c) Reduced HP2 in the presence of DNA; (d) Oxidized HP2 in the presence DNA.

Conclusion

We described Zn(II) binding to a series of peptides representing partial sequences of human protamine HP2. DNA precipitation by these peptides and the effects of Zn(II) thereon were investigated as well. The results enabled us to suggest possible binding sites for Zn(II) in the whole HP2 molecule under various conditions. The major conclusion emerging from these investigations is that HP2 may exhibit heterogeneity of Zn(II) binding *in vivo*. Zn(II) enhanced DNA precipitation by all partial peptides. This effect indicates that Zn(II) may participate in the physiological regulation of sperm chromatin condensation. However, more definitive data regarding the positions and coordination modes of the Zn(II) binding sites and their physiological significance to sperm chromatin structure can be only provided by future studies under conditions securing solubility of the DNA-protamine complexes.

Acknowledgements

This work was supported by the Polish Committee for Scientific Research (KBN) grant no. 6 P04A 024 13 and grant no. SPUB/COST/T-9/DZ 44/99, within the framework of the COST D8 action. A subsistence grant from Fogarty International Center, National Institutes of Health, USA, to W.B. and a Domestic Grant for Young Scholars from the Foundation of Polish Science to M.D. are also gratefully acknowledged.

Reference

1. McKay DJ, Renaux BS, Dixon GH: Human sperm protamines. Amino-acid sequences of two forms of protamine P2. Eur J Biochem 156: 5–8, 1986
2. Ammer H, Henschen A, Lee CH: Isolation and amino-acid sequence analysis of human sperm protamines P1 and P2. Occurrence of two forms of protamine P2. Biol Chem Hoppe-Seyler 367: 515–522, 1986
3. Pogany GC, Corzett M, Weston S, Balhorn R: DNA and protein content of mouse sperm. Exp Cell Res 136: 127–136, 1981
4. Balhorn R, Reed S, Tanphaichitr N: Aberrant protamine 1/protamine 2 ratios in sperm of infertile human males. Experientia 44: 52–55, 1988
5. Bjorndahl L, Kvist U: Influence of seminal vesicular fluid on the zinc content of human sperm chromatin. Int J Androl 13: 232–237, 1990
6. Bench G, Corzett MH, Kramer CE, Grant PG, Balhorn R: Zinc is sufficiently abundant within mammalian sperm nuclei to bind stoichiometrically with protamine 2. Mol Reprod Dev 56: 512–519, 2000
7. Gatewood JM, Schroth GP, Schmid CW, Bradbury EM: Zinc-induced secondary structure transitions in human sperm protamines. J Biol Chem 265: 20667–20672, 1990
8. Bianchi F, Rousseaux-Prevost R, Sautiere P, Rousseaux J: P2 protamines from human sperm are zinc-finger proteins with one Cys2/His2 motif. Biochem Biophys Res Commun 182: 540–547, 1992
9. Quintanilla-Vega B, Hoover DJ, Bal W, Silbergeld E, Waalkes MP, Anderson LD: Lead interaction with human protamine HP2 as a mechanism of male reproductive toxicity. Chem Res Toxicol 13: 594–600, 2000
10. Kozlowski H, Bal W, Dyba M, Kowalik-Jankowska T: Specific structure-stability relations in metallopeptides. Coord Chem Rev 184: 319–346, 1999
11. Bal W, Jeżowska-Bojczuk M, Kasprzak KS: Binding of nickel(II) and copper(II) to the N-terminal sequence of human protamine HP2. Chem Res Toxicol 10: 906–914, 1997
12. Bal W, Lukszo J, Kasprzak KS: Mediation of oxidative DNA damage by nickel(II) and copper(II) complexes with the N-terminal sequence of human protamine HP2. Chem Res Toxicol 10: 915–921, 1997
13. Liang R, Senturker S, Shi X, Bal W, Dizdaroglu M, Kasprzak KS: Effects of Ni(II) and Cu(II) on DNA interaction with the N-terminal sequence of human protamine P2: Enhancement of binding and mediation of oxidative DNA strand scission and base damage. Carcinogenesis 20: 893–898, 1999
14. Bal W, Wójcik J, Maciejczyk M, Grochowski P, Kasprzak KS: Induction of a secondary structure in the N-terminal pentadecapeptide of human protamine HP2 through Ni(II) coordination. An NMR study. Chem Res Toxicol 13: 823–830, 2000
15. Bianchi F, Rousseaux-Prevost R, Bailly C, Rousseaux J: Interaction of human P1 and P2 protamines with DNA. Biochem Biophys Res Commun 201: 1197–1204, 1994
16. Krizek BA, Merkle DL, Berg JM: Ligand variation and metal ion binding specificity in zinc finger peptides. Inorg Chem 32: 937–940, 1993
17. Berg JM, Godwin HA: Lessons from zinc-binding peptides. Annu Rev Biophys Biomol Struct 26: 357–371, 1997
18. Meienhofer J, Waki M, Heimer EP, Lambros TJ, Makofske RC, Chang CD: Solid phase synthesis without repetitive hydrolysis. Preparation of leucylalanyl-glycyl-valine using 9-fluorenylmethyloxy- carbonylamino acids. Int J Peptide Prot Res 13: 35–42, 1979
19. Irving H, Miles MG, Pettit LD: A study of some problems in determining the stoichiometric proton dissociation constants of complexes by potentiometric titrations using a glass electrode. Anal Chim Acta 38: 475–488, 1967
20. Gans P, Sabatini A, Vacca A: SUPERQUAD: An improved general program for computation of formation constants from potentiometric data. J Chem Soc Dalton Trans 1195–1199, 1985
21. Lees WJ, Whitesides GM: Equilibrium constants for thiol-disulfide interchange reactions: A coherent, corrected set. J Org Chem 58: 642–647, 1993
22. Krężel A, Leśniak W, Jeżowska-Bojczuk M, Młynarz P, Brasuń J, Kozłowski H, Bal W: Coordination of heavy metals by dithiothreitol, a commonly used thiol group protectant. J Inorg Biochem 84: 77–88, 2001
23. Banerjea D, Kaden T, Sigel H: Enhanced stability of ternary complexes in solution through the participation of heteroaromatic N bases. Comparison of the coordination tendency of pyridine, imidazole, ammonia, acetate and hydrogen phosphate toward metal ion nitrilotriacetate complexes. Inorg Chem 20: 2586–2590, 1981
24. Vu HM, Minch MJ: α-(Ac)AKRHRKV, a model of the histone H4 amino terminus, uses an unprotonated histidine in phosphate binding. J Pep Res 51: 162–170, 1998
25. Woody RW: Circular dichroism and conformation of unordered peptides. Adv Biophys Chem 2: 37–79, 1992
26. Roehm PC, Berg JM: Sequential metal binding by the RING finger domain of BRCA1. Biochemistry 36: 10240–10245, 1997
27. Basile LA, Coleman JE: Optical activity associated with the sulfur to metal charge transfer bands of Zn and Cd GAL4. Prot Sci 1: 617–624, 1992.
28. Vašák M, Kägi JHR, Hill HAO: Zinc(II), cadmium(II) and mercury(II) thiolate transitions in metallothionein. Biochemistry 20: 2852–2856, 1981
29. Worthington MT, Amann BT, Nathans D, Berg JM: Metal binding properties and secondary structure of the zinc-binding domain of Nup475. Proc Natl Acad Sci USA 93: 13754–13759, 1996
30. Posewitz MC, Wilcox DE: Properties of the Sp1 zinc finger 3 peptide: Coordination chemistry, redox reactions, and metal binding competition with metallothionein. Chem Res Toxicol 8: 1020–1028, 1995
31. Predki PF, Sarkar B: Effect of replacement of 'zinc finger' zinc on estrogen receptor DNA interactions. J Biol Chem 267: 5842–5846, 1992
32. Fita I, Campos JL, Puigjaner LC, Subirana, JA: X-ray diffraction study of DNA complexes with arginine peptides and their relation to nucleoprotamine structure. J Mol Biol 167: 157–177, 1983
33. Balhorn R: A model for the structure of chromatin in mammalian sperm. J Cell Biol 93: 298–305, 1982
34. Hud NV, Milanovich FP, Balhorn R: Evidence of novel secondary structure in DNA-bound protamine is revealed by Raman spectroscopy. Biochemistry 33: 7528–7535, 1994
35. Wallace TJ, Schriesheim A: Solvent effects in the base-catalyzed oxidation of mercaptans with molecular oxygen. J Org Chem 27: 1514–1516, 1962
36. Kvist U: Importance of spermatozoal zinc as temporary inhibitor of sperm nuclear chromatin decondensation ability in man. Acta Physiol Scand 109: 79–84, 1980

37. Bjorndahl L, Kjellberg S, Roomans GM, Kvist U: The human sperm nucleus takes up zinc at ejaculation. Int J Androl 9: 77–80, 1986
38. Kvist U, Bjorndahl L, Kjellberg S: Sperm nuclear zinc, chromatin stability, and male fertility. Scanning Microsc 1: 241–1247, 1987
39. Kvist U, Kjellberg S, Bjorndahl L, Soufir JC, Arver S: Seminal fluid from men with agenesis of the Wolffian ducts: Zinc-binding properties and effects on sperm chromatin stability. Int J Androl 13: 245–252, 1990
40. Balhorn R, Corzett M, Mazrimas JA: Formation of intraprotamine disulfides *in vitro*. Arch Biochem Biophys 296: 384–393, 1992
41. Zalensky AO, Allen MJ, Kobayashi A, Zalenskaya IA, Balhorn R, Bradbury EM: Well-defined genome architecture in the human sperm nucleus. Chromosoma 103: 577–590, 1995
42. Allen MJ, Bradbury EM, Balhorn R: AFM analysis of DNA-protamine complexes bound to mica. Nucleic Acids Res 25: 2221–2226, 1997
43. Brewer, LR, Corzett M, Balhorn R: Protamine-induced condensation and decondensation of the same DNA molecule. Science 286: 120–123, 1999